JACS
JOURNAL OF THE AMERICAN CHEMICAL SOCIETY

Communication

pubs.acs.org/JACS

Amorphous Hierarchical Porous GeO_x as High-Capacity Anodes for Li Ion Batteries with Very Long Cycling Life

Xiao-Liang Wang,[†] Wei-Qiang Han,*[,†] Haiyan Chen,[‡,#] Jianming Bai,[§,∥] Trevor A. Tyson,[‡] Xi-Qian Yu,[⊥] Xiao-Jian Wang,[⊥] and Xiao-Qing Yang[⊥]

[†]Center for Functional Nanomaterials, Brookhaven National Laboratory, Upton, New York 11973, United States

[‡]Physics Department, New Jersey Institute of Technology, Newark, New Jersey 07102, United States

[§]Materials Science and Engineering, University of Tennessee, Knoxville, Tennessee 37996, United States

[∥]High Temperature Materials Laboratory, Oak Ridge National Laboratory, Oak Ridge, Tennessee 37831, United States

[⊥]Chemistry Department, Brookhaven National Laboratory, Upton, New York 11973, United States

Supporting Information

ABSTRACT: Many researchers have focused in recent years on resolving the crucial problem of capacity fading in Li ion batteries when carbon anodes are replaced by other group-IV elements (Si, Ge, Sn) with much higher capacities. Some progress was achieved by using different nanostructures (mainly carbon coatings), with which the cycle numbers reached 100−200. However, obtaining longer stability via a simple process remains challenging. Here we demonstrate that a nanostructure of amorphous hierarchical porous GeO_x whose primary particles are ∼3.7 nm diameter has a very stable capacity of ∼1250 mA h g^{-1} for 600 cycles. Furthermore, we show that a full cell coupled with a $Li(NiCoMn)_{1/3}O_2$ cathode exhibits high performance.

There is great interest in developing novel anode materials for high-performance Li ion batteries, which are the key parts of electric vehicles (EVs). The mass deployment of EVs is critical for the whole world to meet our urgent energy challenges.[1−3] Unfortunately, all of the high capacity anode materials (e.g., silicon, germanium, and tin) suffer from the major problem of poor capacity retention, which prevents them from being used in large commercial applications.

In essence, anode volume changes and stresses, concomitant with Li^+ intake/removal, can induce particle cracking/pulverization, which creates new surfaces that consume lithium, cause irreversibility, and form isolated fragments. The volume change can also cause disconnections between the active materials and the current collector, interrupting the charge-transportation pathway and thus engendering isolated parts. This irreversibility and insulation finally translate into a loss in capacity and failure of the battery. To solve this stability problem, researchers have developed multiple approaches, including (i) tolerance enhancement, such as decreasing dimensional size[4] and amorphization;[5] (ii) accommodation, such as pore formation;[6] (iii) buffering, which may involve making composites with carbon and/or inactive components, carbon coating, alloying, thin filming, and modifying binders and the solid electrolyte interface (SEI) layer coating;[7−10] and (iv) limitation, such as narrowing the voltage window and fixing the lithiation level.[11]

Most encouragingly, a few recent reports on tailored nanostructures have documented good cell stability (i.e., high capacities without a discernible decline for at least 100 full cycles).[6,12−16] These nanostructures generally are grouped into two classes: carbon composites and thin films. For example, a hierarchical porous structure of 10−30 nm Si nanoparticles (∼50 wt %) deposited on 15−35 μm chained carbon black particles attained an overall capacity of ∼1500 mA h g^{-1} for 100 cycles.[15]

However, both classes have several disadvantages. In carbon composites (in which the added carbon constituted over half the weight of the composites in some cases), the following drawbacks were evident: (i) the presence of low-capacity carbon suppresses the overall energy density; (ii) the synthesis usually involves multiple complicated steps; (iii) the intact surface coating decreases the electrode's kinetics; and (iv) carbon affords only limited accommodation, so the composites either must be porous to provide preformed voids or require inactive oxides to buffer the volume change, which magnifies the effects of the other three disadvantages. On the other hand, thin films are suitable only for microbatteries, and their performance must be stabilized via thick inactive substrates.

Therefore, searching for an inexpensive, high-performance material without a carbon coating has always been greatly attractive but very challenging. Here we present a simple, cheap, and easily scaled-up synthetic procedure for making GeO_x powders with a high capacity of ∼1250 mA h g^{-1} for 600 cycles when used as anodes. Interestingly, the resulting nanostructure exhibits features of hierarchical porous agglomerates, is amorphous, and contains ∼3.7 nm primary particles that afford us an ideal model system for studying the mechanism whereby this nanostructure exhibits extended cycling in the absence of extra carbon compositing or confinement from substrates. A GeO_x /$Li(NiCoMn)_{1/3}O_2$ full cell also demonstrated excellent capacity retention.

GeO_x powders were prepared by a wet-chemistry route at room temperature, modifying a procedure reported by Jing et

Received: September 28, 2011
Published: December 5, 2011

al.[17] for preparing wormlike crystalline Ge nanostructures. The synthesis began with the formation of germanate ions by the reaction of GeO_2 with NH_4OH, which was followed by reduction of these ions using $NaBH_4$. First, we stirred 8 g of GeO_2 (99.999%, Aldrich) in 144 mL of distilled water. After the addition of 16 mL of NH_4OH (28.0−30.0% NH_3, Alfa), the dispersion became transparent. Next, a fresh $NaBH_4$ (98%, Alfa) solution (14.464 g in 80 mL of water) was injected into the solution, and the mixture was stirred continuously for 20 h. The resulting powder was collected by filtration, washed with distilled water, and dried under vacuum.

The hierarchical porous nanostructure was revealed by scanning electron microscopy (SEM) and transmission electro microscopy (TEM) images (Figure 1a−c). The low-magnification SEM image (Figure 1a) shows micrometer-sized agglomerates containing nanopores. As depicted at higher magnification (Figure 1b), there are ∼50 nm sized nanoagglomerates. With a further increase in magnification using TEM (Figure 1c), the presence of 3.7 ± 1.0 nm primary nanoparticles was observed. Nitrogen absorption measurements determined a Brunauer−Emmett−Teller (BET) surface area of 187 $m^2\ g^{-1}$.

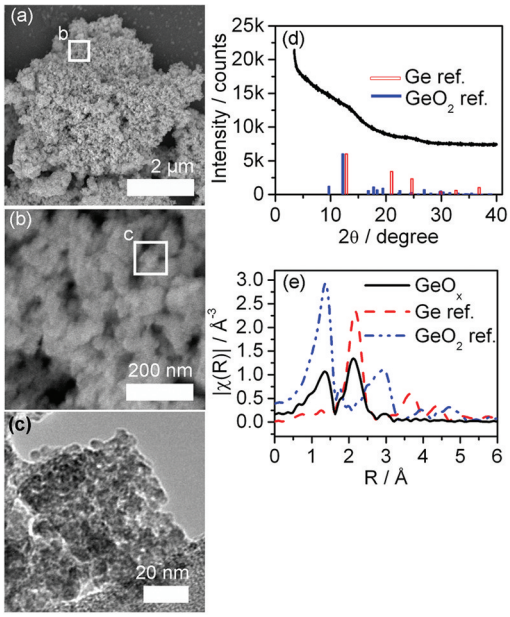

Figure 1. Nano- and atom structure of the initial GeO_x. (a−c) Hierarchical nanoporous structure revealed by (a) a low-magnification SEM image, (b) an enlarged SEM image corresponding to the area enclosed by the square in (a), and (c) a TEM image corresponding to the area in the square in (b). (d) Synchrotron XRD profile (λ = 0.72958 Å). (e) Synchrotron EXAFS profile. Powder diffraction file (PDF) peaks of Ge (no. 00-004-0545) and GeO_2 (no. 01-085-0473) and synchrotron EXAFS data for Ge and GeO_2 references are also shown in (d) and (e), respectively.

High-resolution synchrotron X-ray diffraction (XRD) measurements confirmed the amorphous structure of this material. The XRD profile in Figure 1d illustrates a smoothly declining intensity with increasing 2θ, with only two broad peaks near 13 and 24° and no sharp peaks at all. These two peaks coincide with the Ge(111) and Ge(220) peaks of Ge, respectively. Therefore, the atomic arrangement in GeO_x is more similar to that in Ge. Assuming that the former reflects Ge(111), we estimated the extent of the short-range order as 8 Å using the Scherrer formula.

In addition, scanning TEM−energy-dispersive X-ray spectroscopy (STEM−EDS) indicated the oxygen content to be ∼13 wt %, corresponding to a Ge/O molar ratio of 6:4. Synchrotron extended X-ray absorption fine structure (EXAFS) spectra at the Ge K-edge (Fourier transformed but not phase corrected; Figure 1e) also confirmed the existence of oxygen in the sample. The Ge atoms in this sample form the first coordination shell, with a Ge−Ge bond length similar to that in crystalline Ge, and O atoms form the second coordination shell, with a Ge−O bond length similar to that in GeO_2. Therefore, we denote the sample as GeO_x.

For comparison, we annealed samples in H_2 at 300 and 700 °C for 30 min. The 300 °C sample retained its micrometer-sized agglomerates consisting of ∼20 nm nanoparticles (Figure 2a,b) and was still amorphous (Figure 2e); however, the structure of the 3.7 nm primary particles was lost (Figure 2c). The surface area decreased to 58.3 $m^2\ g^{-1}$. The sample annealed at 700 °C consisted only of solid micrometer-sized crystalline particles (Figure 2d,e).

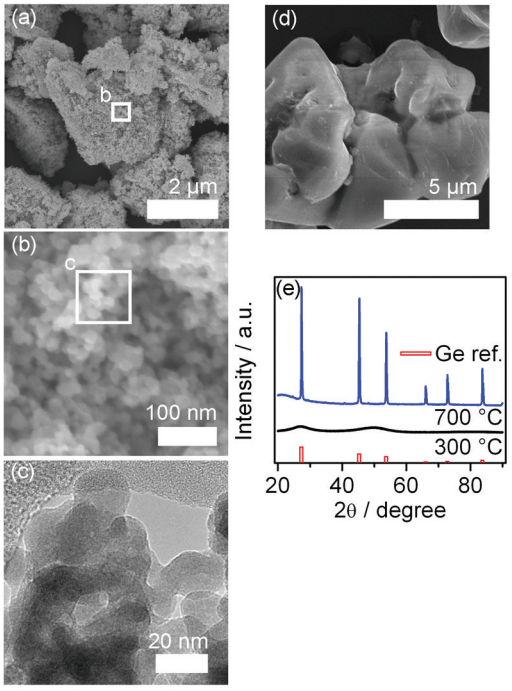

Figure 2. Structures of samples annealed at 300 and 700 °C. (a−c) Nanoporous structure of the 300 °C sample revealed by (a) a low-magnification SEM image, (b) an enlarged SEM image corresponding to the square area in (a), and (c) a TEM image corresponding to the square area in (b). (d) Low-magnification SEM image of the 700 °C sample. (e) XRD profiles (λ = 1.5418 Å). PDF peaks of Ge (no. 00-004-0545) also are depicted.

When employed as an anode material in Li ion batteries, the initial GeO_x sample exhibited very stable cycling behavior with a highly reversible capacity. Anode films consisted of the active material, carbon black (Super P Li, TIMCAL), and a lithium polyacrylate (Li-PAA) binder[18] with a composition of 8:1:1 by weight. The voltage window was from 0.05 to 1.5 V.

As detailed in Figure 3a, its initial C/20 (80 mA g^{-1}) reversible capacity was found to be 1728 mA h g^{-1}. The theoretical capacity for GeO_x (x = 0.67) is 1845 mA h g^{-1}

dx.doi.org/10.1021/ja208880f | J. Am. Chem.Soc. 2011, 133, 20692−20695

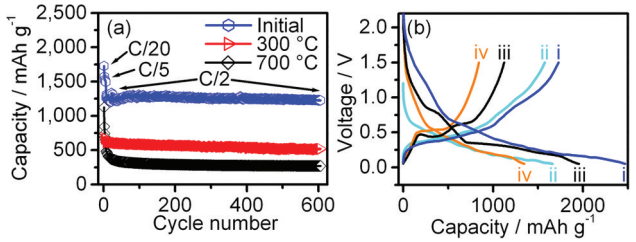

Figure 3. Anode performance in half-cells. (a) Reversible capacities. (b) Charge–discharge curves: (i) first cycle of the initial GeO_x (C/20); (ii) second cycle of the initial GeO_x (C/5); (iii) first cycle of the 700 °C sample (C/20); (iv) second cycle of the 700 °C sample (C/5).

assuming that O participates in Li storage by the reversible formation/decomposition of Li_2O. Afterward, the C/5 and C/2 capacities were found to be 1575 and 1268 mA h g^{-1}, respectively. Impressively, when cycled at the rate of C/2, the anode retained its capacity very well for 600 full charge/discharge cycles. The capacity of the 600th C/2 cycle was still 96.7% of that of the first one. The cycling was quite stable at a higher rate of 2C, as shown in Figure S1 in the Supporting Information.

Increasing size of the amorphous particles (the 300 °C sample) decreased the capacity (i.e., 688 mA h g^{-1} at C/20, 661 mA h g^{-1} at C/5, and 607 mA h g^{-1} at C/2). Nevertheless, the cycling stability was still excellent. Furthermore, along with the diminution in the porous amorphous structure, the anode (cf. the 700 °C sample) behaved like a bulk alloy system: its capacity faded rapidly in the first few cycles and stabilized at a lesser stage. Figure 3b depicts charge–discharge curves of the initial GeO_x sample and the 700 °C sample. It is worth noting that germanium and germanium oxide have different cycling behaviors.[19]

The superior performance of the hierarchical porous GeO_x sample suggested to us that the origin of this high performance (structural stability and reactivity) reflects the synergy of the sample's four characteristics: small primary particles, porous structure, amorphous state, and the incorporation of oxygen. Among them, the small size of primary particles might play a crucial role for the following reasons: (i) It could avoid the widespread problem of pulverization of high-capacity anode materials. Reportedly, micrometer-sized Ge particles used as anodes in Li ion batteries were broken into 5–15 nm particles after some cycles.[20] Because the size of the primary particles in our samples already is only ~3.7 nm, it is hard to envision their further reduction. (ii) The absolute volume change of each single particle is small, which is good for preserving electrical contact as well as the particle's integrity. (iii) Their smallness facilitates the charge transfer (both ionic and electronic) over shorter distances, and having more surfaces for transfer enhances the reactivity. The small primary particle thus is the basis for efficiently maintaining the hierarchical porous structure's stability and integrity upon high-capacity cycling. Growing the particles to 20 nm resulted in lower capacities but still good stability at this level of lithiation (cf. the 300 °C sample).

Besides the very small particles, the amorphous structure is another important factor directly related to a stable capacity. In previous work by others, ultrafine crystallites (<10 nm) still showed high but fading capacities; thus, Kim and Cho reported 76% capacity retention for mesoporous Si with a 6.5 nm crystal size after 50 cycles.[21] Therefore, small crystalline Ge particles presumably could suffer from a similar fading of capacity; possible reasons for this could be the harmful anisotropic expansion/extraction and the stresses accompanying phase transitions upon (de)lithiation in crystalline anodes.

Furthermore, the hierarchical porous structure of the initial GeO_x is useful for preserving intact the micrometer-sized agglomerate morphology. Anode particles, even small amorphous ones, need room for expansion during lithiation. Lack of such preservation might change the microscopic charge-transport pathway and the particles' locations, which could in turn lead to loss in the electrical contact. Another possible scenario is that there only is limited room for expansion, so contractive stresses would be built up and cracks would develop. In comparison, 10 nm amorphous Ge particles were shown only to be stable for 30 cycles at a level of ~1480 mA h g^{-1}; demonstration of their long-term stability is lacking.[22] Therefore, porosity also plays an important role in stabilizing the capacity.

The initial GeO_x has a Barrett–Joyner–Halenda (BJH) pore volume of 0.34 cm^3 g^{-1}. For simplification, we used the density of crystalline Ge to estimate that the pores of a 1 g sample can accommodate an extra 1.81 g of GeO_x, that is, the system can accommodate a 1.81-fold increase in volume. Taking into account the change in the volume of oxygen in our sample, this opening space could well accommodate the volume change. Oxygen could form Li_2O with reversible lithium, as suggested by our selected-area electron diffraction (SAED) patterns. The role of oxygen in this dilution of volume expansion is similar to, for example, that of second metals in alloy anodes and of oxygen in conversion electrodes and alloy-metal oxides.

We noted the preservation of the micrometer-sized agglomerates of the initial GeO_x after running it for lengthy cycles, as is evident in Figure S2. The annealed samples showed much lower (but still stable) capacities. The 300 °C sample was still amorphous and porous and had a similar Ge/O ratio, which stabilized the cell performance. The retention of the agglomerate morphology after cycling is shown in Figure S2b. Its low capacity comes from the larger particle size (20 vs 3.7 nm), indicating that size is critical for reactivity. This low lithiation level also helps stabilize the capacity. The solid micrometer-sized particles annealed at 700 °C underwent cracking/pulverization upon cycling (Figure S2c). Therefore, after the morphology becomes stable, only a small fraction can contribute to the capacity.

To make a practical high-performance anode, we had to surmount the hurdle of low initial Coulombic efficiency (70%). The extent of Li storage irreversibility is typical of systems with high surface areas and results, for example, from the consumption of Li^+ for forming SEIs during lithiation. We tackled this problem by depositing air-stable lithium powder on the anode film (Lectro Max, FMC Lithium). The extra Li ion source helps to compensate for the generation of lithium consumed by the SEI formation and enhances the electrochemical reversibility of the anode. We obtained an initial efficiency of 99.5% with an open-circuit voltage (OCV) of 0.74 V.

Ultimately, evaluating a full-cell performance is a very challenging key step toward its application. The fact that the lithium metal electrode no longer serves both as an abundant Li ion source and as a reference electrode with little potential change upon (de)lithiation crucially tests the real reversibility of the anode.

dx.doi.org/10.1021/ja208880f | J. Am. Chem.Soc. 2011, 133, 20692–20695

We used a $Li(NiCoMn)_{1/3}O_2$ (NCM) cathode and the Li-compensated GeO_x anodes to fabricate full cells. A full cell exhibited a discharge capacity of 164 mA h $(g\ of\ NCM)^{-1}$ at a constant current/constant voltage (CCCV) rate of *C*/20 [based on $Li(NiCoMn)_{1/3}O_2$] between 2.5 and 4.2 V, with an initial 85% Coulombic efficiency (Figure 4a). The voltages were lower

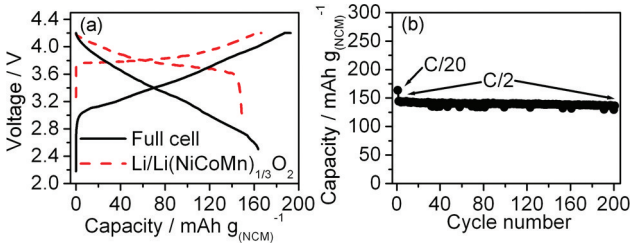

Figure 4. Cell performance of the initial GeO_x anode. (a) Initial profiles of the Li-compensated GeO_x/NCM full cell in comparison with those of the Li metal/NCM half-cell. (b) Reversible battery discharge capacity of NCM in the full cell.

and more slanted than those obtained using lithium metal as the anode (i.e., in the half-cell). The cell realized a capacity of 144 mA h $(g\ of\ NCM)^{-1}$ at the following *C*/2 rate [based on $Li(NiCoMn)_{1/3}O_2$]. Importantly, as shown in Figure 4b, the cycling was stable, with an average loss over 200 cycles of only 0.028% per cycle. Recently, Hassoun et al.[23] reported that their Sn−C composite/$Li(Ni_{0.45}Co_{0.1}Mn_{1.45})O_4$ battery had an initial capacity of 125 mA h $(g\ of\ cathode)^{-1}$ and a loss of ∼0.060% per cycle for 87 cycles. The performance shown by our anode is indicative of its excellent reversibility and stability in a full cell.

■ ASSOCIATED CONTENT

Supporting Information

2*C* performance of the initial GeO_x anode in the half-cell and SEM images of microstructures after cycling. This material is available free of charge via the Internet at http://pubs.acs.org.

■ AUTHOR INFORMATION

Corresponding Author

whan@bnl.gov

Present Address

[#]Mineral Physics Institute and Department of Geosciences, Stony Brook University, Stony Brook, NY 11794.

■ ACKNOWLEDGMENTS

Research was carried out at the Center for Functional Nanomaterials, Brookhaven National Laboratory, which is supported by the U.S. Department of Energy, Office of Basic Energy Sciences, under Contract DE-AC02-98CH10886. This work was also supported by an E-LDRD Fund of Brookhaven National Laboratory. X. J. Wang, X. Q. Yu, and X. Q. Yang were supported by the Assistant Secretary for Energy Efficiency and Renewable Energy, Office of Vehicle Technologies, under the Vehicle Technology Program. We thank Dr. Hong Li (Institute of Physics, Chinese Academy of Sciences) for valuable discussions.

■ REFERENCES

(1) Armand, M.; Tarascon, J. M. *Nature* **2008**, *451*, 652.
(2) Key, B.; Morcrette, M.; Tarascon, J. M.; Grey, C. P. *J. Am. Chem. Soc.* **2011**, *133*, 503.
(3) Zu, C. X.; Li, H. *Energy Environ. Sci.* **2011**, *4*, 2614.
(4) Chan, C. K.; Peng, H. L.; Liu, G.; McIlwrath, K.; Zhang, X. F.; Huggins, R. A.; Cui, Y. *Nat. Nanotechnol.* **2008**, *3*, 31.
(5) Fan, Q.; Chupas, P. J.; Whittingham, M. S. *Electrochem. Solid-State Lett.* **2007**, *10*, A274.
(6) Park, M. H.; Kim, K.; Kim, J.; Cho, J. *Adv. Mater.* **2010**, *22*, 415.
(7) Xing, W. B.; Wilson, A. M.; Eguchi, K.; Zank, G.; Dahn, J. R. *J. Electrochem. Soc.* **1997**, *144*, 2410.
(8) Kepler, K. D.; Vaughey, J. T.; Thackeray, M. M. *Electrochem. Solid-State Lett.* **1999**, *2*, 307.
(9) Guo, J. C.; Chen, X. L.; Wang, C. S. *J. Mater. Chem.* **2010**, *20*, 5035.
(10) Wang, X. L.; Feygenson, M.; Chen, H. Y.; Lin, C. H.; Ku, W.; Bai, J.; Aronson, M. C.; Tyson, T. A.; Han, W. Q. *J. Am. Chem. Soc.* **2011**, *133*, 11213.
(11) Besenhard, J. O.; Yang, J.; Winter, M. *J. Power Sources* **1997**, *68*, 87.
(12) Hassoun, J.; Panero, S.; Simon, P.; Taberna, P. L.; Scrosati, B. *Adv. Mater.* **2007**, *19*, 1632.
(13) Derrien, G.; Hassoun, J.; Panero, S.; Scrosati, B. *Adv. Mater.* **2007**, *19*, 2336.
(14) Yu, Y.; Gu, L.; Wang, C. L.; Dhanabalan, A.; van Aken, P. A.; Maier, J. *Angew. Chem., Int. Ed.* **2009**, *48*, 6485.
(15) Magasinski, A.; Dixon, P.; Hertzberg, B.; Kvit, A.; Ayala, J.; Yushin, G. *Nat. Mater.* **2010**, *9*, 353.
(16) Hertzberg, B.; Alexeev, A.; Yushin, G. *J. Am. Chem. Soc.* **2010**, *132*, 8548.
(17) Jing, C. B.; Zang, X. D.; Bai, W.; Chu, J. H.; Liu, A. Y. *Nanotechnology* **2009**, *20*, No. 505607.
(18) Li, J.; Le, D. B.; Ferguson, P. P.; Dahn, J. R. *Electrochim. Acta* **2010**, *55*, 2991.
(19) Kim, Y.; Hwang, H.; Lawler, K.; Martin, S. W.; Cho, J. *Electrochim. Acta* **2008**, *53*, 5058.
(20) Yoon, S.; Park, C. M.; Sohn, H. J. *Electrochem. Solid-State Lett.* **2008**, *11*, A42.
(21) Kim, H.; Cho, J. *Nano Lett.* **2008**, *8*, 3688.
(22) Lee, H.; Kim, M. G.; Choi, C. H.; Sun, Y. K.; Yoon, C. S.; Cho, J. *J. Phys. Chem. B* **2005**, *109*, 20719.
(23) Hassoun, J.; Lee, K. S.; Sun, Y. K.; Scrosati, B. *J. Am. Chem. Soc.* **2011**, *133*, 3139.